Electronic Properties of the Boron–Oxygen Defect Precursor of the Light-Induced Degradation in Silicon

Zhuangyi Zhou, Michelle Vaqueiro-Contreras, Mattias Klaus Juhl, and Fiacre Rougieux

***Abstract*—In this work, we study the electronic properties of the boron–oxygen precursor defect responsible for light-induced degradation in crystalline silicon via deep-level transient spectroscopy. Even though this degradation has been known for many decades, and has resulted in severe silicon solar cell degradation, its root cause is poorly understood. The detection of a deep defect correlated to BO degradation has only been reported recently using deep-level transient spectroscopy. The resulting trap has been labeled as H390. In this work, we confirm the existence of this trap and report on the observation of a second defect (H400), which appears to be similarly associated with the BO light-induced degradation. To the best of our knowledge, this level has not been previously reported and could result from a second latent form of the BO light-induced degradation defect, a topic that has been largely debated in the literature. The concentration of both levels increases following dark annealing and decreases following minority carrier injection. The two levels disappear during BO activation and appear during BO deactivation, confirming a link between the observed levels and the latent state of the BO defect. Furthermore, consistent with previous studies, the two traps are metastable and change configurations after hole capture. Finally, we determine the minority carrier capture cross-section of the active BO defect by comparing the latent defect concentration with the minority carrier lifetime.**

***Index Terms*—BO-LID, crystalline silicon, DLTS, defect, degradation, p-type silicon.**

I. Introduction

LIGHT-INDUCED degradation (LID) of boron-doped silicon crystals used in photovoltaics has been studied for many decades. Such degradation can lead to $\sim 2\%_{\text{abs}}$ degradation of conversion efficiencies and substantial energy loss in solar panels based on boron-doped silicon [1]. Passivated emitter rear cells and aluminum back-surface field cells made of boron-doped Czochralski silicon (Cz-Si) suffer from BO-LID, and such degradation also affects other materials, such as quasi-mono and multicrystalline silicon [2]. This degradation results from carrier injection from either above-band gap illumination [3] (e.g., sunlight) or forward electrical bias [4]. It was found that such degradation scales linearly with the boron concentration and has a quadratic relation to the oxygen concentration of the material [5]. The degradation is thus largely accepted to result from boron and oxygen atom interactions [6], presumably in a $B_s O_2$ configuration as suggested from *ab initio* calculations [7]–[9]. Although, some other authors have proposed a Si self-interstitial with an acceptor complex as the responsible defect, with supporting experimental and *ab initio* calculations [10]. This LID is referred to as BO-LID, to differentiate it from other types of light/carrier-induced degradation mechanisms affecting silicon wafers [11]. Experimental work using lifetime spectroscopy has led to the development of a three-state model (A: latent, B: activated, and C: stabilized) for the BO-LID defect [12]. The corresponding defect reaction kinetics, namely activation/deactivation kinetics (A $\leftrightarrow$ B), regeneration/redegradation kinetics (B $\leftrightarrow$ C), and stabilization/destabilization kinetics (A $\leftrightarrow$ C), have been largely studied in the literature [3], [5], [6], [12]–[18]. Nevertheless, most of the electrical characterization of the defect has relied on indirect methods, predominately being lifetime spectroscopy. Due to some challenges brought by the nature of this defect, detection of its electrical signature via capacitance spectroscopy methods had not been reported until recently. A trap associated with the "latent" form of the recombination active BO defect has now been detected via deep-level transient spectroscopy (DLTS) and reported in the literature [8]. The activation energy for hole emission of the identified deep donor trap has been reported and confirmed in this work to be 0.97 eV via junction capacitance methods. It is proposed that such a trap, herein labeled as H375 (labeled as H390 in [8]), corresponds to the "annealed" state of the BO defect and is not recombination active.

In this work, an additional level is observed via DLTS measurements. We show that the manifestation and defect concentrations of these two "latent" levels are correlated. The effective defect density extracted from photoconductance measurements and the trap concentration measured via DLTS are anticorrelated. This anticorrelation allows us to extract the minority capture cross-section of the recombination active BO defect. Furthermore, we observe an unusual decrease in the trap concentration upon long filling pulse excitation during capture measurements, indicating possible configuration changes of the defect during carrier injection. A possible explanation for the missed observation of this trap in previous studies [8] and [9] is the requirement of unusual measurement parameters (high

Manuscript received 17 May 2022; revised 24 June 2022; accepted 8 July 2022. Date of publication 25 July 2022; date of current version 19 August 2022. This work was supported in part by the Australian Research Council (ARC) Discovery Early Career Researcher Award (DECRA) project under Grant DE160101368, in part by the Australian Renewable Energy Agency (ARENA) under Grant 2017/RND003, and in part by the Australian Centre for Advanced Photovoltaics (ACAP) projects under Grant 1-SRI001 and Grant RG200768-B. *(Corresponding author: Michelle Vaqueiro-Contreras.)*

The authors are with the School of Photovoltaic and Renewable Energy Engineering, University of New South Wales, Sydney, NSW 2033, Australia (e-mail: zhuangyi.zhou@unsw.edu.au; m.vaqueirocontreras@unsw.edu.au; mattias.juhl@unsw.edu.au; fiacre.rougieux@unsw.edu.au).

Color versions of one or more figures in this article are available at https://doi.org/10.1109/JPHOTOV.2022.3190769.

Digital Object Identifier 10.1109/JPHOTOV.2022.3190769

temperatures and extended filling pulse times), and potentially the thermal history of the studied samples which is known to affect the presence of the fast and slow forming BO-related defect [19].

II. Experiment Methodology

We have studied B-doped Cz-Si crystals with a resistivity of 3.5 Ω·cm and an oxygen concentrations of $8.7 \times 10^{17} \pm 7 \times 10^{16}$ cm^{-3} according to Fourier transform infrared spectroscopy measurements. The wafers were RCA cleaned and diffused in a clean furnace with a phosphorus solid source at 950° C for 1 h while the measured sheet resistance is 70 Ω/sq. After phosphorus diffusion, one side of the sample was protected with a photoresist and the other side was etched in a mixture of HNO_3 (70%):HF (49%):H_2O = 25:1:25 to remove the diffused layer. The samples were annealed in a clean furnace at 700° C for 20 min to eliminate the impact of thermal donors [20] on the lifetime and the DLTS measurements. The samples were cleaved into smaller pieces adequate for lifetime and DLTS measurements. The single-side diffused lifetime samples were then passivated with a 20-nm amorphous silicon (a-Si) layer on each side. The a-Si layers were deposited at 300° C for 30 s using an Oxford Instruments plasmalab 100 PECVD system. n^+p diodes were fabricated for DLTS measurements for which the Si samples were first dipped in HF prior to contact evaporation to remove the oxide. Au was thermally evaporated on the rear (etched) side to form back contacts. Al was thermally evaporated on the front (diffused) side as front contacts. Then, the Au side was fully protected by the photoresist while the Al side was covered with ∼ 1-mm diameter dot-patterned photoresist. Finally, the samples were etched with the same mixed solution of HNO_3 (70%):HF (49%):H_2O = 25:1:25 to form mesa diodes. At the same time, a sample of 5 Ω·cm B-doped FZ silicon was used as control and was processed into a n^+p diode for DLTS measurements using the same fabrication process. All DLTS measurements were carried out using a HERA DLTS tool from PhysTech. The carrier lifetime measurements were realized using quasi-steady-state photoconductance (QSSPC) measurements with a photoconductance tool (Sinton Instruments, WCT-120TS [21]).

In order to evaluate the presence of the BO defect in the material, the lifetime samples were illuminated with a 1 kW/m^2 white light phosphor-based LED lamp, with 1.78×10^{17} cm^{-2}s^{-1} absorbed photon flux, at room temperature for 24 h. After the degradation, the characteristic recovery of the BO-LID was recorded after a 200° C anneal without illumination. In the case of the DLTS samples, measurements were performed on as-manufactured diodes, after minority carrier injection for defect activation and after dark anneal for deactivation (recovery). Minority carrier injection was performed *in situ* using a forward bias of 2.5 V applied on the n^+p junction for up to 80 h, leading to the formation of the recombination active state of the BO defect. For BO deactivation the samples were also annealed *in situ* in dark at 420 K for up to 100 min, which is the upper limit of our available setup but still enough to deactivate the defect given long enough time [13], [16]. For the capture kinetics analysis

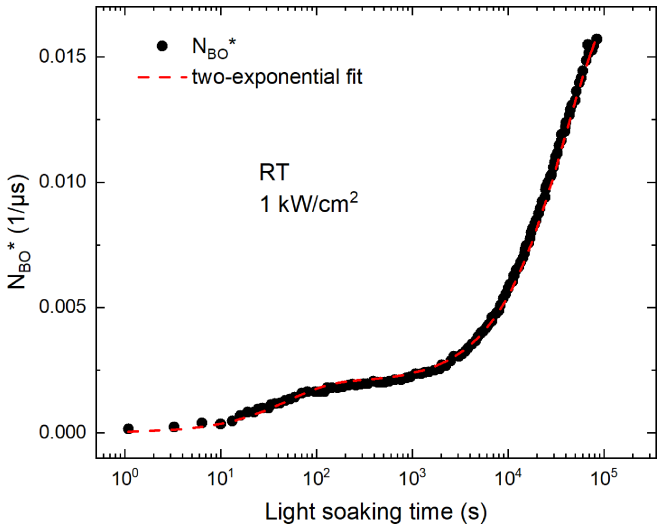

Fig. 1. Normalized defect density of BO [N_{BO}^*] as a function of light soaking time at room temperature of a 3.5 Ω· cm B-doped p-type Cz silicon sample (extracted at an injection level $\Delta n = 1 \times 10^{14}$ cm^{-3}). The red dashed line is a double exponential fit of the measured data.

between DLTS traps and lifetime-extracted defect density, we studied the BO-deactivation kinetics of both sets of samples. For such measurement, we used the same 420-K dark annealing conditions given the setup limitations.

The normalized defect density of BO (N_{BO}^*) was calculated from the lifetime measurements at an injection level of 1×10^{14} cm^{-3} using

$$N_{BO}^* = \frac{1}{\tau_{BO}(X)} = \frac{1}{\tau_{deg}(X)} - \frac{1}{\tau_{ann}(X)} \quad (1)$$

where X is the accumulated time under illumination, τ_{deg} is the lifetime at degraded state, and τ_{ann} is the lifetime after BO deactivation. Throughout the formation and deactivation of the BO defect, the concentration of various traps was monitored with DLTS using the height of the DLTS peak as a proxy for concentration [22].

III. Results

In Fig. 1, results from the normalized BO defect density (N_{BO}^*) monitored throughout a degradation process using the QSSPC technique are shown. The formation kinetics of the degraded state BO defect can be fitted with a double exponential arising from the characteristic two-stage degradation mechanism of BO-LID [3], [13], [14], and [16]. Following the degradation, the sample was annealed in the dark at 200° C. This process recovered the sample's lifetime to its initial effective lifetime in the low injection range ($\leq 10^{14}$ cm^{-3}), as expected from BO-LID (see Fig. 2), and rules out Cu-related LID [23]. We also performed a Fe–B pair dissociation check using QSSPC for which our samples showed no changes in the lifetime [24] and therefore indicating that Fe was below the detectable amounts. From these results, we can conclude that the BO-LID defect is present in the studied material, and it is not affected by other types of commonly encountered LID mechanisms in silicon.

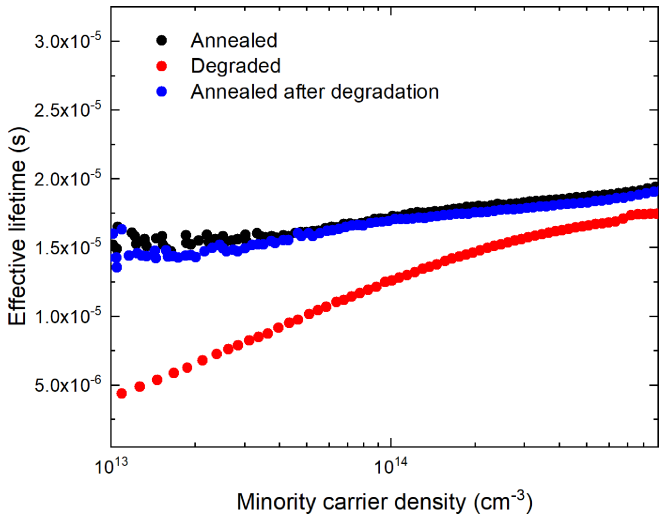

Fig. 2. Minority carrier lifetime of the sample in Fig. 1 as annealed, degraded, and annealed again after the degradation.

DLTS measurements were then performed *in situ* after minority carrier injection and dark annealing processes. Fig. 3(a) shows some of the DLTS spectra from these measurements on a diode on its as-manufactured state, after minority carrier injection, and after dark anneal. These DLTS scans were performed at a temperature range from 295 to 410 K, applying a long filling pulses needed for the observation of the deep donor trap. The measurement details are provided in the figure. Two peaks are observed, the first at about 375 K and the other at a higher temperature near 400 K. In the same figure we include the DLTS scan from a B-doped FZ sample used as a reference for comparison, as expected, it is shown that the trap density of the sample is below the detection limit given the low [O] of FZ silicon. Similarly, in order to rule out the influence of other oxygen-related defects, DLTS spectra were also measured in the more standard low-temperature range (20–300 K); no other traps were detected [see Fig. 3(b)]. From these observations, we can conclude that the observed 375- and 400-K peaks seem to be B- and O-related, but unlikely to be related to thermal donor nor other O-related complexes. Analysis of the emission transients at 400 K further reveals the existence of the two traps, namely H375 and H400, with hole emission activation energies 0.97 and 1.65 eV, respectively (see Fig. 4). Note that these two traps were also observed in a 1 Ω·cm and a 5 Ω·cm B-doped Cz samples (not shown). The hole emission energies were extracted from the T^2-corrected Arrhenius plot. The defect concentrations of H375 and H400 have been calculated based on the capacitance–voltage and transient measurements of the diodes. It has been assumed that the filling pulse is sufficiently long to completely fill the two traps. The defect density was calculated according to [25]

$$\frac{\Delta C}{C_0} = \frac{N_t}{2N_d} \tag{2}$$

where ΔC is the DLTS signal, C_0 is the initial capacitance without bias applied, N_t is the defect concentration, and N_d is the background dopant density.

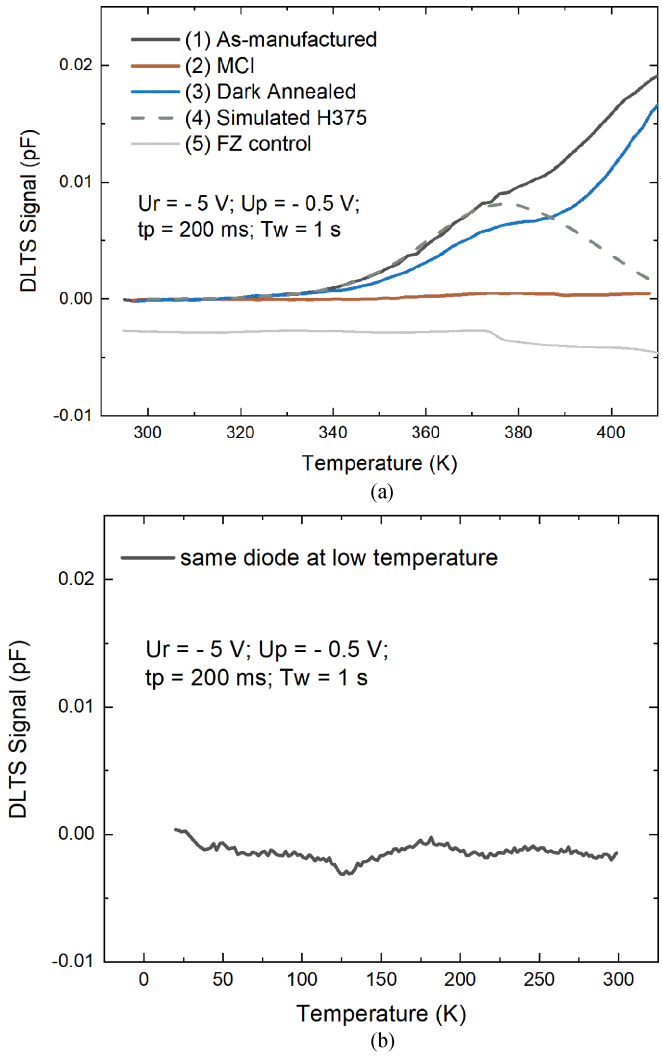

Fig. 3. (a) DLTS spectra from a n^+p diode made from a 3.5 Ω·cm B-doped p-type Cz silicon crystal at different stages (1) as-manufactured, (2) after 320-K forward bias (+2.5 V) for 80 h, (3) after annealing in the dark at 420 K for 100 min with zero bias, (4) simulated spectrum based on the defect properties extracted from [8] with 1-s Tw; and (5) B-doped FZ silicon sample (shifted for clarity). (b) Low-temperature DLTS scans (20–300 K) on the same n^+p diode. DLTS measurement parameters [reverse bias voltage (Ur), filling pulse voltage (Up), filling pulse lengths (tp), and period width (Tw)] are shown in the figures.

The defect concentration and electronic properties of H375 and H400 are summarized in Table 1. Our results indicate that H375 is analogous to the H390 trap reported by Vaqueiro-Contreras *et al.* [8] and it is associated with the latent state of the BO defect. The difference of peak locations in the temperature scale between the defect reported here (375 K) and that by Vaqueiro-Contreras *et al.* (390 K) arises from the difference in measurement conditions, specifically, the time taken after the pulse before the capacitance is measured (Tw). We have included the simulated DLTS spectra of the H390 peak previously reported in Fig. 3(a) using our tool measurement conditions to demonstrate its equivalent position in our measurements. It is important to note the activation energy reported is not the energy level of the trap (the change in the Gibbs free energy),

TABLE I
DEFECT PARAMETERS OF THE H375 AND H400 TRAPS IN SILICON

Defect levels	Vaqueiro-Contreras et al. [8]	H375	H400
E_t+E_∞ (eV)	0.97	0.97	1.65
Arrhenius pre-exponential factor ($s^{-1}K^{-2}$)	1.99×10^8	1.81×10^8	1.57×10^{16}
Defect concentration (cm^{-3})	$> 5 \times 10^{12}$	4.10×10^{12}	1.60×10^{13}
Capture cross section (cm^2)	-	1.07×10^{-21}	4.10×10^{-23}

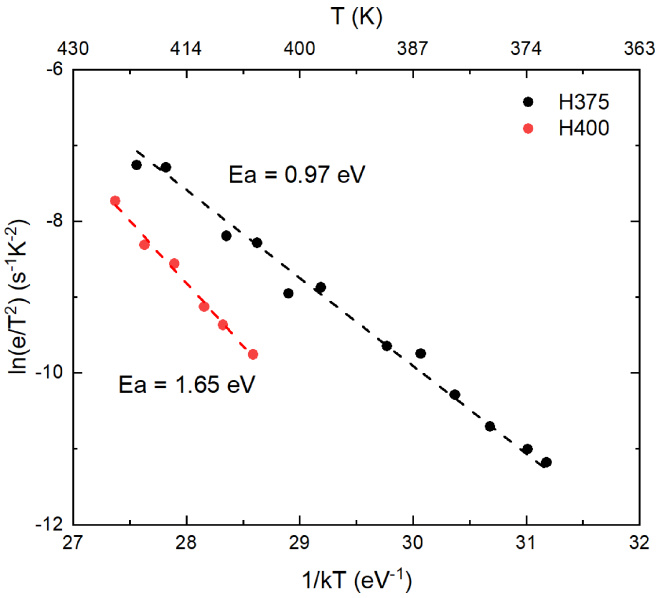

Fig. 4. Arrhenius plot of T^2-corrected emission rates of H375 and H400. The dashed line is a linear fit of the corresponding measured emission.

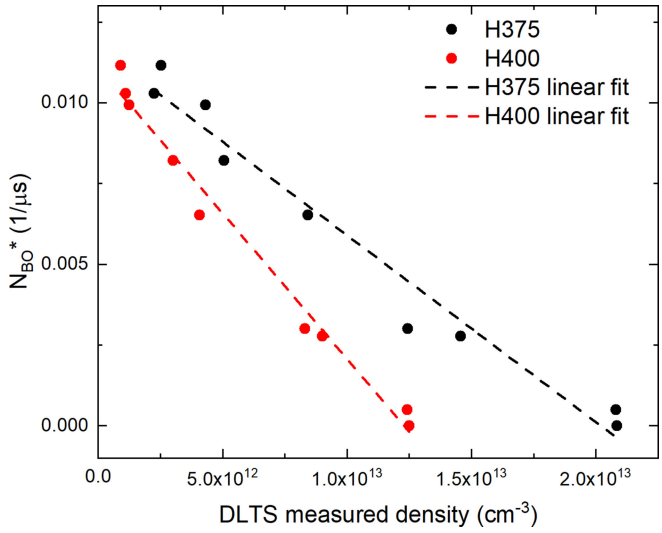

Fig. 5. Comparison between effective lifetime extracted at an injection level of $\Delta n = 1 \times 10^{14}$ cm^{-3} via QSSPC, and the defect density of H375 and H400 via DLTS during accumulated dark anneal at 420 K for 300 min. The dashed line is a linear fit indicating the inverse correlation of BO defect and H375, H400, respectively.

but instead an apparent energy. Typically the measured apparent energy is larger than the change in the Gibbs free energy as the apparent energy includes the thermal activation energy of the majority carrier's capture cross-section. This means that the energy calculated from the Arrhenius plot, as in this case, can lead to energies greater than E_g. Such values which represent activation energies, should not be used with Shockley–Read–Hall recombination statistics for this reason.

To determine if there is an association between H375 and H400 with the BO-LID latent defects, we now compare the defect concentration of H375 and H400 from DLTS in the normalized defect concentration of the BO defect from lifetime spectroscopy. The results are shown in Fig. 5. The defect density of H375 and H400 increases during dark anneal, while the $N_{BO}{}^*$ decreases. Both H375 and H400 form linear correlations with the $N_{BO}{}^*$, strongly suggesting the association. To confirm that H375 and H400 are related to each other, we additionally monitored their defect density using *in situ* DLTS measurements during BO-LID activation and deactivation processes. The defect density of H375 and H400 was monitored during a dark anneal at 420 K (BO regeneration process), while H375 and H400 traps removal was performed by minority carrier injection using a 2.5-V bias (BO degradation process). The results are shown in Fig. 6. We observe that the rates in activation and deactivation of both defects are similar, suggesting that multiple traps are involved in the latent state of the BO recombination active defect.

In order to accurately measure the capture rates of H375 and H400, the change in capacitance resulting from each trap as a function of filling pulse (t_p) was measured, as illustrated in Fig. 7. The amplitudes of H375 and H400 were separated using Laplace DLTS technique [26] on each transient taken after each filling pulse. The measurements were taken at 400 K as it was where the transients of both traps could be clearly observed. As a result, a very unusual drop of the capacitance change of H375 and H400 was observed when the applied filling pulse t_p was greater than ~0.1 and 1 s, respectively, as shown in Fig. 7. A typical majority carrier capture process driven by reverse bias results in the increase of transient magnitudes until saturation (i.e., full occupancy). However, in this particular case, our results indicate that these levels disappear after a long enough filling pulse application. Furthermore, we observe a remarkably similar rate of decay in the H375 transient to that of the H400 increase at $t_p > 0.1$ s, leading to a possible interpretation of configuration changes whereby the defect giving rise to H375 changes into the one introducing H400. Given the unusual behavior of these traps during characterization, it is challenging to precisely calculate the defect densities of the traps, so we summarize the average measured value over the temperature range of 370–410 K and 400–420 K on each of them in Table 1. A possible explanation for the lower concentration of H400 with respect to H375 in Fig. 6 is that the occupancy ratio between H375 and H400 is temperature dependent.

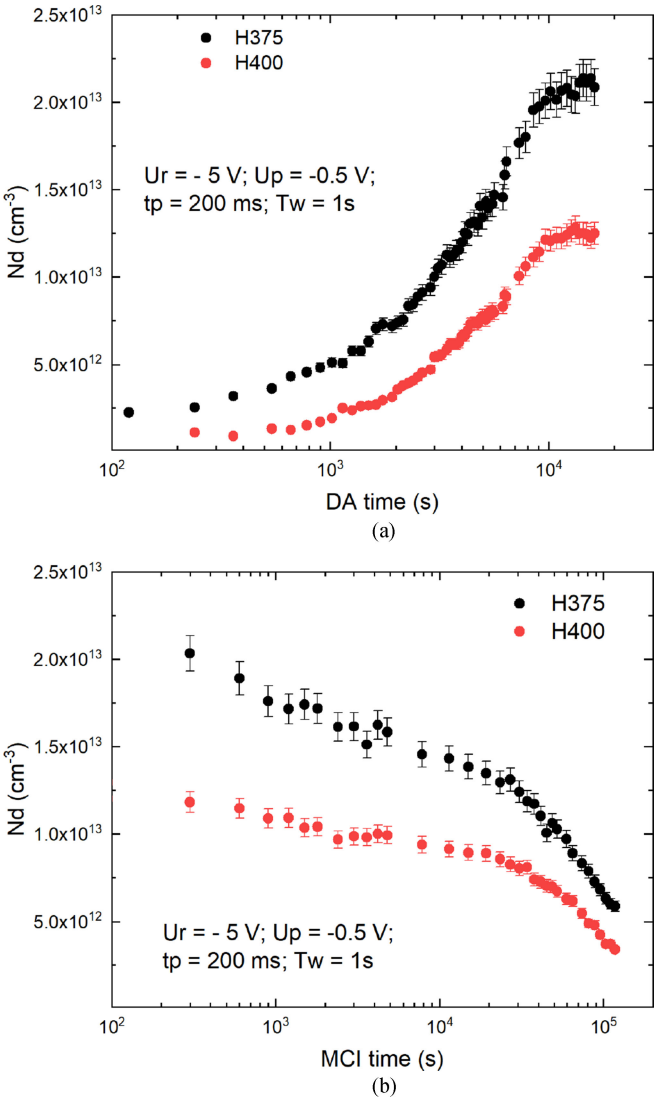

Fig. 6. Trap concentration changes of H375 and H400 during (a) accumulated dark anneal at 420 K and (b) dark MCI (+2.5-V bias) measured at 400 K. The rest of the DLTS measurement parameters are listed in the graph.

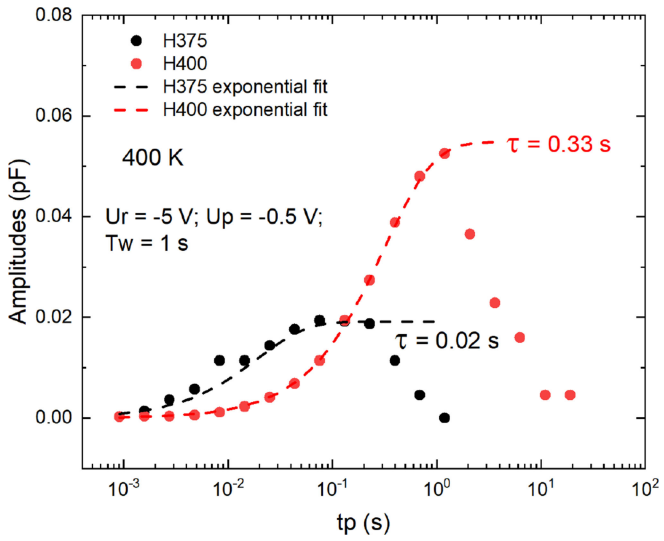

Fig. 7. Capture kinetics of holes from the H375 and H400 traps at 400 K. The dashed lines are a monoexponential fit of the capture processes. DLTS measurement parameters are included in the figure.

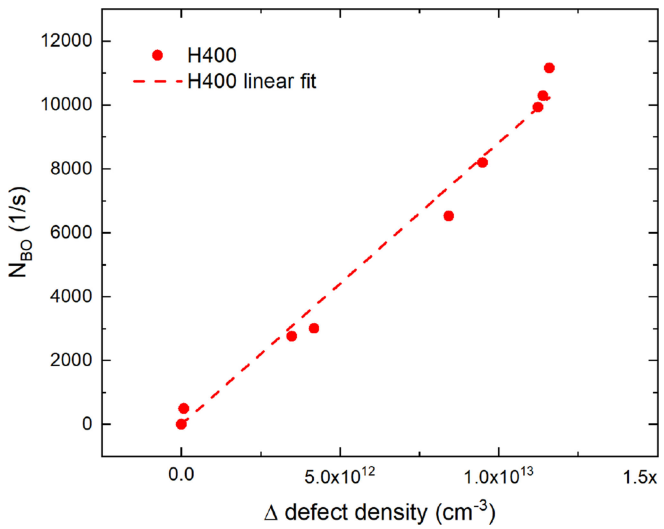

Fig. 8. Linear relationships between N_{BO} (at $\Delta n = 1 \times 10^{14}$ cm^{-3} and 420 K), and the sum defect density of H375 and H400. The dashed line is a linear fit with 0 as the intercept.

We have estimated the capture cross-section for minority carriers of the BO-LID defect using the extracted recombination rates from lifetime measurements and the defect concentration from DLTS measurements. To do this, we assume the recombination active state of BO-LID defects completely transforms into the latent states H375 and H400 via deactivation annealing. The capture cross-section of electrons can be derived from the combination of (1) and the Shockley–Read–Hall equation at low injection

$$\frac{1}{\tau_{\mathrm{BO}}(x)} = N_t \sigma_e v_{\mathrm{th}} \tag{3}$$

where x is the accumulated time under dark anneal; N_t is the recombination active defect density, σ_e is the electron capture cross-section, and v_{th} is the thermal velocity of electrons. $N_{t(\mathrm{BO})}$ is the recombination active BO defect density, which is calculated as the maximum trap concentration (H375 plus H400) minus the trap concentration at time t: $N_{t(\mathrm{BO})} = N_{\mathrm{H375+H400,max}} - N_{\mathrm{H375+H400},t}$. This predicts a linear relationship between N_{BO} and the defect density increase of H375 and H400, inline with what we found during the dark anneal, as shown in Fig. 8. The data presented in Fig. 8 thus represents the product of σ_e and v_{th} at 420 K. This allows the determination of the electron capture cross-section of the recombination active BO state assuming the direct transfer to H375 and H400 to be calculated as 4.45×10^{-17} cm^2, which agrees with the previously predicted value by Mchedlidze *et al.* [27].

IV. Discussion

The BO-LID defect(s) formation kinetics has been thoroughly studied in the literature, however, due to the limitations of the methods used there is still a rather dramatic debate about its true identity [18]. Amongst some theories and observations; Hashigami *et al.* [3] and Bothe *et al.* [13] have suggested the existence of two BO recombination centres, which are commonly referred to as the fast recombination center (FRC) and the slow recombination center (SRC). The rates $R_{\text{deg, FRC}}$ and $R_{\text{deg, SRC}}$ are typically several orders of magnitude apart from each other [16], [18], which have been observed to occur sequentially or simultaneously [18].

Even though many authors have considered the two stages of the degradation as the result of two different defects [16], [18], some have suggested otherwise. Hallam *et al.* [15] proposed that BO-LID was due to only one type of defect, and speculated that the FRC stage could be caused by the activation of a defect precursor (from the latent state to the activated state), whereas SRC arises from the transformation of a species to the latent state. This is also similar to what Nærland *et al.* [28] has described, with the determination of a two-hole capture process as rate-limiting for BO-LID formation. Nevertheless, Bothe *et al.* [29] and [30] observed that the FRC activation could be triggered or suppressed via the different forward voltage applied for current-induced degradation, whereas the SRC was formed in the same way, indicating that the two defects' formation was decoupled.

More recently, however, Schmidt *et al.* [18] have proposed a reconciliation of the available formation theories and described a few models from literature as well as from their own observations. Two of these models include the "sequential" and "parallel" mechanisms, depicted in the model proposed by Herguth *et al.* [12], which suggests the existence of two latent states of the same or different defects leading to the staged degradation. Many of these degradation stages can be affected by the thermal history of the sample. For example, after a very short (in the order of a few seconds) dark anneal only the FRC is observed, whereas after a longer anneal (minutes) a two-stage degradation dominated by the SRC is observed [3], [13], [14], [16]. From our observations, and in particular, from the results shown in Fig. 7, we suggest the involvement of two latent defects in the degradation. Presumably, two latent defects of the same composition but of different configuration.

V. Conclusion

In this work, we report the observation and characterization of two trap levels via DLTS that have an anticorrelated formation relationship to that of the BO-LID in B-doped Cz silicon. The negative linear correlation between the recombination active BO centres and the measured trap concentrations suggests these are precursors to the BO-LID defect. We report the activation energies and capture properties of the two traps. Using extended filling pulses, we observe unusual capture behaviors that the capacitance drops, which we attribute to configuration changes, although more work is required to fully understand the captured behavior. It is argued that our results support the idea of having two latent defects precursors for the degradation, which has been a topic of extensive debate in the literature for many years.

Acknowledgements

The views expressed herein are not necessarily the views of the Australian Government, and the Australian Government does not accept responsibility for any information or advice contained herein.

References

[1] K. Arafune et al., "Study on defects and impurities in cast-grown polycrystalline silicon substrates for solar cells," *Phys. B: Condens. Matter*, vol. 376–377, pp. 236–239, 2006.
[2] J. Lindroos and H. Savin, "Review of light-induced degradation in crystalline silicon solar cells," *Sol. Energy Mater. Sol. Cells*, vol. 147, pp. 115–126, 2016.
[3] H. Hashigami, Y. Itakura, and T. Saitoh, "Effect of illumination conditions on Czochralski-grown silicon solar cell degradation," *J. Appl. Phys.*, vol. 93, no. 7, pp. 4240–4245, 2003.
[4] K. Bothe, R. Hezel, and J. Schmidt, "Recombination-enhanced formation of the metastable boron-oxygen complex in crystalline silicon," *Appl. Phys. Lett.*, vol. 83, no. 6, pp. 1125–1127, 2003.
[5] J. Schmidt and K. Bothe, "Structure and transformation of the metastable boron- and oxygen-related defect center in crystalline silicon," *Phys. Rev. B*, vol. 69, Jan. 2004, Art. no. 024107.
[6] S. Glunz, S. Rein, W. Warta, J. Knobloch, and W. Wettling, "Degradation of carrier lifetime in CZ silicon solar cells," *Sol. Energy Mater. Sol. Cells*, vol. 65, no. 1, pp. 219–229, 2001.
[7] M. Sanati and S. K. Estreicher, "Temperature and sample dependence of the binding free energies of complexes in crystals: The case of acceptor-oxygen complexes in Si," *Phys. Rev. B*, vol. 72, Oct. 2005, Art. no. 165206, doi: 10.1103/PhysRevB.72.165206.
[8] M. Vaqueiro-Contreras et al., "Identification of the mechanism responsible for the boron oxygen light induced degradation in silicon photovoltaic cells," *J. Appl. Phys.*, vol. 125, no. 18, 2019, Art. no. 185704.
[9] V. P. Markevich et al., "Boron-oxygen complex responsible for light-induced degradation in silicon photovoltaic cells: A new insight into the problem," *Phys. Status Solidi (A)*, vol. 216, no. 17, 2019, Art. no. 1900315.
[10] C. Möller and K. Lauer, "Light-induced degradation in indium-doped silicon," *Phys. Status Solidi (RRL)-Rapid Res. Lett.*, vol. 7, no. 7, pp. 461–464, 2013.
[11] J. Lindroos, A. Zuschlag, J. Carstensen, and G. Hahn, "Light-induced degradation variation in industrial multicrystalline PERC silicon solar cells," *AIP Conf. Proc.*, vol. 1999, no. 1, 2018, Art. no. 130013.
[12] A. Herguth and G. Hahn, "Kinetics of the Boron-oxygen related defect in theory and experiment," *J. Appl. Phys.*, vol. 108, no. 11, 2010, Art. no. 114509.
[13] K. Bothe and J. Schmidt, "Electronically activated Boron-oxygen-related recombination centers in crystalline silicon," *J. Appl. Phys.*, vol. 99, no. 1, 2006, Art. no. 0 13701.
[14] V. Voronkov, R. Falster, K. Bothe, B. Lim, and J. Schmidt, "Lifetime-degrading boron-oxygen centres in p-type and n-type compensated silicon," *J. Appl. Phys.*, vol. 110, no. 6, 2011, Art. no. 063515.
[15] B. Hallam, M. Abbott, T. Nærland, and S. Wenham, "Fast and slow lifetime degradation in boron-doped Czochralski silicon described by a single defect," *Phys. Status Solidi (RRL)-Rapid Res. Lett.*, vol. 10, no. 7, pp. 520–524, 2016.
[16] T. Niewelt, J. Schön, W. Warta, S. W. Glunz, and M. C. Schubert, "Degradation of crystalline silicon due to boron-oxygen defects," *IEEE J. Photovolt.*, vol. 7, no. 1, pp. 383–398, Jan. 2017.
[17] B. Hallam et al., "Eliminating light-induced degradation in commercial p-type Czochralski silicon solar cells," *Appl. Sci.*, vol. 8, no. 1, 2018, Art. no. 10.
[18] J. Schmidt, K. Bothe, V. V. Voronkov, and R. Falster, "Fast and slow stages of lifetime degradation by boron-oxygen centers in crystalline silicon," *Phys. Status Solidi (B)*, vol. 257, no. 1, 2020, Art. no. 1900167.
[19] M. Kim et al., "Modulating the extent of fast and slow boron-oxygen related degradation in Czochralski silicon by thermal annealing: Evidence of a single defect," *J. Appl. Phys.*, vol. 121, no. 5, 2017, Art. no. 053106.

[20] Y. Tokuda, N. Kobayashi, A. Usami, Y. Inoue, and M. Imura, "Thermal donor annihilation and defect production in n-type silicon by rapid thermal annealing," *J. Appl. Phys.*, vol. 66, no. 8, pp. 3651–3655, 1989.
[21] R. A. Sinton and A. Cuevas, "A quasi-steady-state open-circuit voltage method for solar cell characterization," in *Proc. 16th Eur. Photovol. Solar Energy Conf.*, 2000, vol. 1152, Art. no. 4.
[22] D. Lang, H. Grimmeiss, E. Meijer, and M. Jaros, "Complex nature of gold-related deep levels in silicon," *Phys. Rev. B*, vol. 22, no. 8, 1980, Art. no. 3917.
[23] A. Inglese, J. Lindroos, and H. Savin, "Accelerated light-induced degradation for detecting copper contamination in p-type silicon," *Appl. Phys. Lett.*, vol. 107, no. 5, 2015, Art. no. 052101.
[24] D. Macdonald et al., "Formation rates of iron-acceptor pairs in crystalline silicon," *J. Appl. Phys.*, vol. 98, no. 8, 2005, Art. no. 083509.
[25] J. Orton and P. Blood, *The Electrical Characterization of Semiconductors: Majority Carriers and Electron States*. New York, NY, USA: Academic, 1992.
[26] L. Dobaczewski, P. Kaczor, I. Hawkins, and A. Peaker, "Laplace transform deep-level transient spectroscopic studies of defects in semiconductors," *J. Appl. Phys.*, vol. 76, no. 1, pp. 194–198, 1994.
[27] T. Mchedlidze and J. Weber, "Direct detection of carrier traps in Si solar cells after light-induced degradation," *Phys. Status Solidi (RRL)-Rapid Res. Lett.*, vol. 9, no. 2, pp. 108–110, 2015.
[28] T. U. Nærland et al., "Studying light-induced degradation by lifetime decay analysis: Excellent fit to solution of simple second-order rate equation," *IEEE J. Photovolt.*, vol. 3, no. 4, pp. 1265–1270, Oct. 2013.
[29] K. Bothe and J. Schmidt, "Fast-forming boron-oxygen-related recombination center in crystalline silicon," *Appl. Phys. Lett.*, vol. 87, no. 26, 2005, Art. no. 262108.
[30] K. Bothe, "Oxygen-related trapping and recombination centres in borondoped crystalline silicon," Ph.D. dissertation, Leibniz Universität Hannover, 2006.